

OPTICAL AND INFRARED REFLECTANCE OF METAL-INSULATOR COMPOSITES*

N. E. Russell, E. M. Yam and D. B. Tanner
The Ohio State University, Columbus, Ohio 43210

ABSTRACT

The reflectance in the infrared and visible (0.08 eV to 3.2 eV) has been measured for aluminum small particles compacted into potassium chloride. The aluminum particles were prepared by evaporation in inert gas atmosphere and had mean diameters of 200 \AA and 600 \AA . The volume fraction, f , of metal in the samples studied was between $f = 0.03$ and $f \sim 1$. For $f \sim 0.15$ the specimens exhibited finite dc conductivity. The main feature of the data is a decreasing reflectance with increasing frequency. The magnitude of the reflectance increases with metal concentration. Comparison of experiment with simple theories shows that the self consistent theory predicts the general form of the reflectance if the low concentration for first achieving conduction is taken into consideration. Kramers-Kronig inversion of the reflectances yield frequency dependent conductivities which are not like those of a simple metal.

INTRODUCTION

There has been some disagreement in the literature recently over the dielectric function appropriate to describe the optical properties of composite systems. In particular Stroud¹ has proposed that the effective medium approximation² (EMA) should be used while Gittleman and Abeles³ have advocated use of the Maxwell-Garnett theory⁴ (MGT).

EXPERIMENT

We have measured the reflectance in the visible and infrared of composite systems formed by compacting together small particles of aluminum and KCl. The particles were made by the smoke method: evaporating aluminum in an argon atmosphere. Argon pressure was about 0.2 Torr to produce $d \sim 200\text{\AA}$ particles and 0.5 Torr giving $d \sim 600\text{\AA}$ particles.

The particles were thoroughly mixed with KCl powder, $40\text{ }\mu\text{M} < d < 100\text{ }\mu\text{M}$, pressed into a disk shaped pellet and mounted into a grating spectrometer for reflectance measurements. Four gratings were used to cover 600 cm^{-1} to 26000 cm^{-1} (0.075 eV to 3.25 eV) with thermocouple, lead sulfide and photomultiplier detectors as appropriate.

Figure 1 shows the reflectance of $d \sim 200\text{\AA}$ aluminum particles, of volume fraction $f = 0.03$, $f = 0.18$ and $f = 0.30$ metal. The low

concentration shows a rather flat reflectance. The two higher concentrations show a high low frequency reflectance which falls rapidly as the frequency is increased. The general shape of the reflectance is characteristic of a poor conductor. This is consistent with the observation that both of these samples were conducting, with $\sigma \sim 1\Omega^{-1}\text{cm}^{-1}$

Figure 2 shows the reflectance of composites made from $d \sim 600\text{\AA}$ Al particles in KCl with $f = 0.03$, $f = 0.50$, $f = 0.75$ and $f \approx 1$. The $f \sim 1$ sample was prepared in the same way as the others except that no KCl was used. The concentration is not known very accurately. The sample looks like rather old aluminum foil and is quite brittle. The shapes of the reflectances are similar to those in Figure 1 while the magnitudes are somewhat lower. Because the pellets used in these measurements were reground and repressed five to ten times, these samples were more thoroughly mixed than those whose reflectance is shown in Figure 1.

THEORY

The EMA dielectric function ϵ_{EMA} , arises

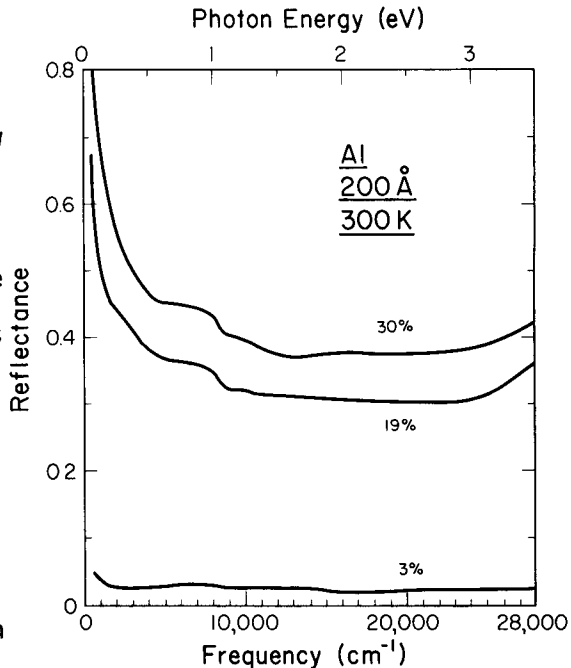


Fig. 1. Reflectance of three concentrations of aluminum particles in KCl.

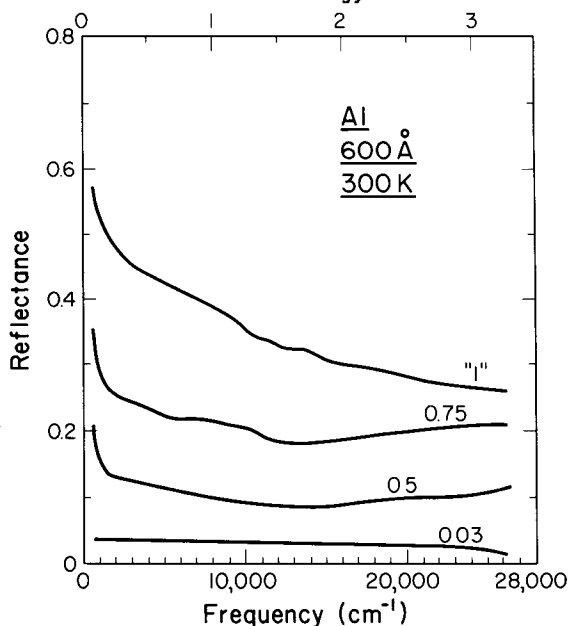


Fig. 2. Reflectance of four aluminum small particle composites.

from the solution of a quadratic equation which, assuming spherical particles, is:

$$f \frac{\epsilon_{\text{EMA}} - \epsilon_A}{2\epsilon_{\text{EMA}} + \epsilon_A} + (1-f) \frac{\epsilon_{\text{EMA}} - \epsilon_B}{2\epsilon_{\text{EMA}} + \epsilon_B} = 0 \quad (1)$$

where ϵ_A is the dielectric function of one of the components, say the metal, of volume fraction f , and ϵ_B is the dielectric function of the insulator, of volume fraction $(1-f)$. The EMA has the appealing feature of treating both the A and B particles on an equivalent basis. It predicts a metal-insulator transition at metal volume fraction $f = 1/3$. (The observed transitions occur between $f = 0.15$ and $f = 0.6$)

The MGT dielectric function for spherical particles is

$$\epsilon_{\text{MGT}} = \epsilon_B + \epsilon_B \frac{3f(\epsilon_A - \epsilon_B)}{(1-f)\epsilon_A + (2+f)\epsilon_B} \quad (2)$$

with the definitions given above. The MGT treats the type A (metal, usually) particles as being embedded in a uniform background of type B. There is no metal-insulator transition below $f = 1$, although some authors interchange the A and B particles as the metal concentration increases.

If a metal dielectric function is used for type A:

$$\epsilon_A = 1 - \frac{\omega_p^2}{\omega^2 + i\omega/\tau} \quad (3)$$

the MGT predicts an absorption maximum at

$$\omega_0 = \omega_p / \left(1 + \frac{2+f}{1-f} \epsilon_B\right)^{1/2} \quad (4)$$

the so-called Maxwell-Garnett resonance frequency. For $\omega > \omega_0$ the MGT dielectric function is characteristic of a metal while for $\omega < \omega_0$, ϵ_{MGT} is insulator-like. At low concentrations the EMA gives the same result as the MGT. As f increases the EMA predicts the absorption peak broadening and shifting to lower frequencies, reaching $\omega = 0$ at $f = 1/3$.

DISCUSSION

Figure 3 shows the calculated reflectance of composite systems within both the EMA and MGT. This figure should be compared with the measurements shown in Figure 1. For the metal we have used a

Drude dielectric function with parameters appropriate to aluminum at 300K. For the insulator we have used a frequency independent dielectric constant $\epsilon_i = 2.1$. The dielectric is taken to be the host in the MGT. For $f = 0.03$ the two theories produce essentially the same result at these frequencies: a constant low reflectance governed by the insulator dielectric constant. The resonance frequency of equation (4) is $\omega_0 = 50000 \text{ cm}^{-1}$ (6.3 eV). For the higher concentrations the two theories produced qualitatively different results.

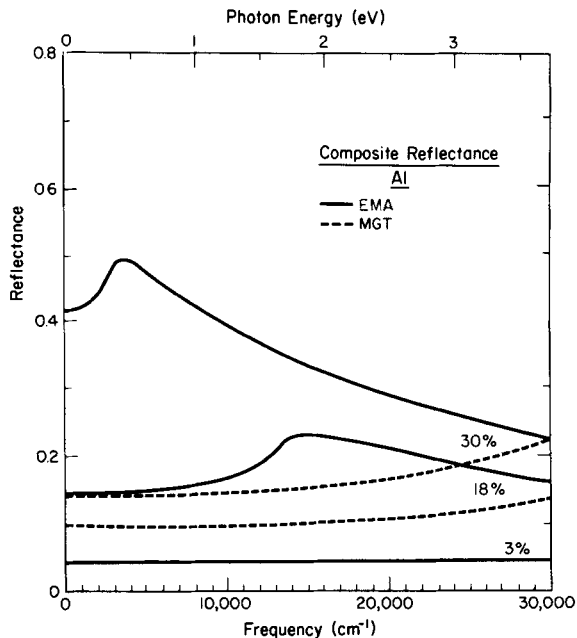


Fig. 3. Calculated reflectance.

The MGT (dashed line) is small at low frequency and rises at high frequencies. The EMA is higher than the MGT at low frequency, produces a weak maximum in the infrared, and then decreases with increasing frequency. The maximum shifts to lower frequency and higher reflectance as the metal concentration increases, reaching zero frequency and unity at $f = 1/3$ (the percolation transition). Since the samples shown in Figure 1 are conducting, the absence of a peak in the measured reflectance should not be surprising. Before any detailed comparison of experiment with theory can be attempted, a theory is needed which either (1) predicts the percolation transition correctly from the structure of the samples or (2) uses experimentally determined percolation parameters as input.

No attempt has been made to fit the reflectance measurements shown in Figure 2. Instead a Kramers-Kronig⁵ analysis of the reflectance was performed. In calculating the integral the measured reflectance was extrapolated to zero frequency using a Hagen-Reubens form: $R \sim 1 - A\omega^{1/2}$ with A chosen such that a smooth connection to experiment was made. At high frequencies a $1/\omega^2$ followed by a $1/\omega^4$ extrapolation was used. Figure 4 shows the frequency dependent conductivity $\sigma_1(\omega) = \omega\epsilon_2(\omega)/4\pi$, where ϵ_2 is the imaginary part of the dielectric function, as determined by the Kramers-Kronig analysis. The important feature of $\sigma_1(\omega)$, which is independent of the

extrapolation procedure, is the broad peak. The peak shifts to lower frequency and the magnitude of the conductivity increases with metal volume fraction. The shift to lower frequency is reminiscent of the EMA behavior in Figure 3, but at high concentrations the MGT resonance, equation (4), also goes down in frequency. The zero frequency intercept of $\sigma_1(\omega)$ is consistent in order of magnitude with rather crude dc resistance measurements ($\sigma \sim 1\text{-}100 \Omega^{-1} \text{cm}^{-1}$).

ACKNOWLEDGMENTS

We have had many useful conversations with and assistance in computer programming from Prof. David Stroud. We thank Prof. F. P. Dickey for the kind loan of the spectrometer.

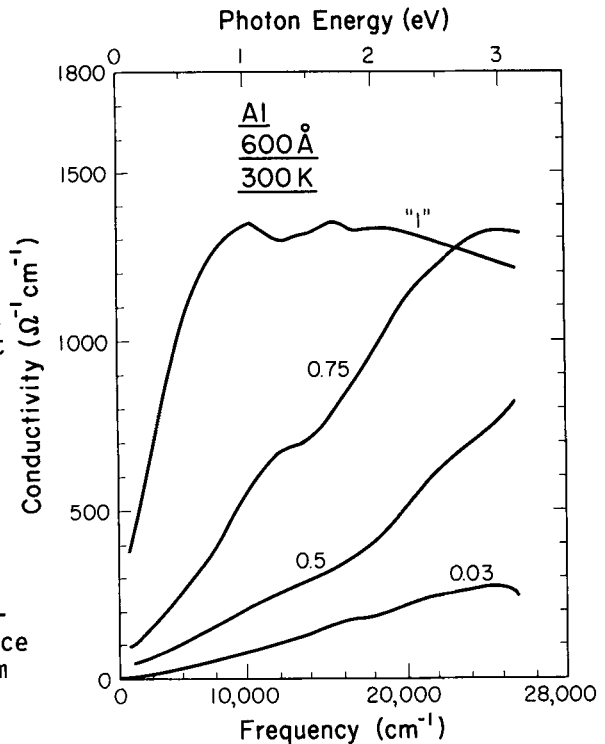


Fig. 4. Kramer-Kronig derived conductivities.

REFERENCES

*Research supported by The Ohio State Program for Energy Research, Education and Public Service.

1. D. Stroud, Phys. Rev. B12, 3368 (1975).
2. D. A. G. Bruggeman, Ann. Phys. (Leipz.) 24, 636 (1935).
3. J. I. Gittleman and B. Abeles, Phys. Rev. B15, 3272 (1977).
4. J. C. Maxwell-Garnett, Philos. Trans. Roy. Soc. A203, 385 (1904).
5. Frederick Wooten, Optical Properties of Solids (Academic Press, 1972), Appendix G.